Published in final edited form as:
Environ Res. 2011 November ; 111(8): 1046–1053. doi:10.1016/j.envres.2011.08.012.

Geostatistical exploration of spatial variation of summertime temperatures in the Detroit metropolitan region

Kai Zhang[a,b,*], **Evan M. Oswald**[c], **Daniel G. Brown**[d], **Shannon J. Brines**[d], **Carina J. Gronlund**[a], **Jalonne L. White-Newsome**[a], **Richard B. Rood**[c], and **Marie S. O'Neill**[a,b]

[a]Department of Environmental Health Sciences, University of Michigan, Ann Arbor, MI, USA

[b]Department of Epidemiology, University of Michigan, Ann Arbor, MI, USA

[c]Department of Atmospheric, Oceanic, and Space Sciences, University of Michigan, Ann Arbor, MI, USA

[d]School of Natural Resources and Environment, University of Michigan, Ann Arbor, MI, USA

Abstract

Background—Because of the warming climate urban temperature patterns have been receiving increased attention. Temperature within urban areas can vary depending on land cover, meteorological and other factors. High resolution satellite data can be used to understand this intra-urban variability, although they have been primarily studied to characterize urban heat islands at a larger spatial scale.

Objective—This study examined whether satellite-derived impervious surface and meteorological conditions from multiple sites can improve characterization of spatial variability of temperature within an urban area.

Methods—Temperature was measured at 17 outdoor sites throughout the Detroit metropolitan area during the summer of 2008. Kriging and linear regression were applied to daily temperatures and secondary information, including impervious surface and distance-to-water. Performance of models in predicting measured temperatures was evaluated by cross-validation. Variograms derived from several scenarios were compared to determine whether high-resolution impervious surface information could capture fine-scale spatial structure of temperature in the study area.

Results—Temperatures measured at the sites were significantly different from each other, and all kriging techniques generally performed better than the two linear regression models. Impervious surface values and distance-to-water generally improved predictions slightly. Restricting models to days with lake breezes and with less cloud cover also somewhat improved the predictions. In addition, incorporating high-resolution impervious surface information into cokriging or universal kriging enhanced the ability to characterize fine-scale spatial structure of temperature.

[*]Corresponding author at: Department of Environmental Health Sciences, University of Michigan, Ann Arbor, MI, USA. Fax: +1 734 936 7283. zhangkai@umich.edu (K. Zhang).

The authors declare they have no competing financial interests.

Conclusions—Meteorological and satellite-derived data can better characterize spatial variability in temperature across a metropolitan region. The data sources and methods we used can be applied in epidemiological studies and public health interventions to protect vulnerable populations from extreme heat events.

Keywords

Geostatistics; Impervious surface; Kriging; Spatial interpolation; Temperature

1. Introduction

Improved characterization of urban microclimates is critical for better understanding the urban heat hazard caused by urban heat islands as well as a warming climate. Previous studies of urban climate have been conducted to explore spatial differences in urban and urban/rural temperatures using either the networks of weather stations or temperature sensors designed specifically for field studies. Temperatures measured in regulatory weather stations have high quality and long time periods, but field studies with temperature sensors have the advantage of flexible sampling locations capturing location-specific characteristics. For example, by comparing temperatures measured in both urban and rural sites in Baltimore and Phoenix, Brazel et al. (2000) reported that the urban–rural minimum temperature gradients had increased and they were positively associated with population change. Harlan et al. (2006) found that neighborhoods in Phoenix with high building density, less vegetation and open space experienced increased temperatures. Oka (2011) suggested that human heat comfort levels in Philadelphia were a function of urban street characteristics, surface materials and time of a day. Finally, Houet and Pigeon (2011) used an automated method to classify and map Urban Climate Zones and compare the temperature data measured in the field to satellite-derived surface temperature in these zones.

Several interpolation methods have been examined to predict the spatial variation of temperature using temperature data from networks of thermometers sited at airports and other locations across a geographic area, often an urban settlement or metropolitan region. The idea behind these methods is that temperature measured at particular points can provide information about the temperatures at points where direct measurements are not available. Methods used to interpolate among these measured points to create a smooth spatial surface of temperature, or to estimate temperatures at nearby locations, include kriging, inverse distance weighting methods, regression methods (Vicente-Serrano et al., 2003), an interpolation optimization method (Loubier, 2007), smoothing splines (Luo et al., 1998), and spatial-temporal modeling (Im et al., 2009). Secondary information related to temperature has also been incorporated into these techniques to improve estimation, including such variables as distance to water bodies (Im et al., 2009), topographic and geographic variables such as elevation, longitude and latitude (Vicente-Serrano et al., 2003), solar radiation (Ninyerola et al., 2000), quantitative climate/meteorological model predictions (Degaetano and Belcher, 2006) and satellite-derived information such as land surface temperature (Vogt et al., 1997).

Satellite images have the advantage of providing continuous geographic coverage of environmental variables, often providing fine scale (e.g., 30 by 30 m resolution) data over large geographic areas. Remote sensing data have been successfully applied in public and environmental health studies in past decades, and can play a critical role in improving our understanding of the relationships between environmental factors and human health, including mitigating risks caused by heat waves (Wilhelmi et al., 2004; NRC, 2007). Rapid development of remote sensing technologies has improved availability of high-resolution land-cover information (USGS, 2011). Land surface temperature is an indicator of the thermal inertia of surface characteristics, and is derived from remotely sensed thermal infrared data by a series of calibrations and conversions accounting for atmospheric mixing (Johnson et al., 2009; Kestens et al., 2011). Impervious surfaces, which are paved or covered with built structures through which water cannot penetrate, contribute to heat accumulation in built-up areas (U.S. EPA, 2008). Imperviousness, usually measured as percent impervious surface covered in a given area, is a useful satellite-derived indicator of land cover. Both land surface temperature and imperviousness have been explored within the context of urban climate or extreme heat exposures. For example, Johnson et al. (2009) and Kestens et al. (2011) demonstrated the significance of land surface temperature in predicting heat-related mortality and exposures. Thermometer measurements are typically made at low spatial density compared to the fine-scale impervious surface data that can be obtained from satellite land-cover images that cover a complete region. However, to the best of our knowledge, previous studies have not examined whether satellite-derived surface information on imperviousness can improve the estimation of temperature or capture the fine-scale spatial structure of temperature in a large area.

This paper examines how impervious surface and meteorological conditions (cloud cover and lake breezes) can be incorporated in geostatistical methods to improve temperature predictions, and characterize fine-scale spatial structure of temperatures in the Detroit metropolitan area. This paper is part of an ongoing research project designed to evaluate heat wave preparedness and sustainability issues in Detroit. In a companion paper, Oswald et al. (submitted for publication) examined the urban heat island of Detroit from a meteorological perspective.

2. Methods

2.1. Data collection

This study was conducted in the Detroit metropolitan area in August 2008. The population of Detroit is 81% African–American, and 26% of its residents live below the poverty level (Schulz and Northridge, 2004). Previous studies in Detroit have shown that individuals with diabetes, with less education and blacks O'Neill et al., 2005 experience disproportionate temperature and mortality impacts (O'Neill et al., 2003, 2005; Schwartz et al., 2004). A recent study of 107 U.S. communities (Anderson and Bell, 2009) shows that Detroit was above the 80th percentile of cities in the increase in mortality risk with daily mean temperature, suggesting that Detroit is strongly affected by heat compared to other cities.

HOBO data loggers (HOBO Pro V2 External Temperature/Relative humidity Data Logger U23-002; HOBO is a registered trademark of Onset Computer Corp., Bourne, MA, USA)

were deployed at 17 sites in the yards of resident volunteers to characterize the variability of temperature throughout the Detroit metropolitan area, Michigan, USA (Fig. 1). Sites were chosen to represent a wide range of impervious surface conditions, measured using local mean percent impervious surface in the vicinity of the residences of participants. A HOBO monitor includes temperature and humidity sensors within naturally aspirated radiation shields and a data logger. These sensors were mounted to thin wooden stakes, and then were placed around 2 m above ground level. HOBO monitors were sited in yards over grass, and away from driveways to minimize microclimate impacts. Our HOBO sitting protocol aimed to ensure that the measurements of these monitors captured variations in neighborhood land-cover conditions, rather than in surface conditions immediately under or near the sensors.

Measurements from all 17 HOBOs were available from August 9 to August 30, 2008. Measurements of temperature and relative humidity were collected on these days at 5-minute intervals and used to conduct the analysis. Three temperature metrics were used: temperatures measured at 5:00 a.m. (Eastern Daylight Time (EDT)) and 5:00 p.m. (EDT), and daily mean temperatures. The 5:00 a.m. and 5:00 p.m. temperature observations were reasonable approximations of daily minimum and maximum values, respectively. Four missing values were replaced using linear interpolation based on values recorded at the same station immediately before and after the missing values. Secondary information including impervious surfaces and distances to the nearest water body were also used in the data analysis. The Detroit metropolitan area is surrounded by three large water bodies: Lake St. Clair, Lake Erie and the Detroit River. Distance-to-water was calculated as the shortest straight line distance between a HOBO site and the Detroit River, Lake Erie or Lake St. Clair (no smaller inland lakes were considered) using ArcGIS 9.1 (ESRI, Redlands, CA).

Imperviousness data (30×30 m) were downloaded from the National Land Cover Database (NLCD) 2006 impervious surface (USGS, 2011). To reduce the computational burden in cokriging, the original 30 m pixel values were averaged at an 800×800 m grid resolution across the study area using ArcGIS 9.1.

Clear days and days with a lake breeze event during daytime were determined based on weather observations downloaded from the National Climatic Data Center (NCDC, 2008). Using cloud cover and rain information from Detroit Metropolitan Wayne County Airport, clear days were defined as days when cloud cover was non-existent or scattered for more than 60% of the daylight hours, and no precipitation occurred. A lake-breeze event was defined as a day in which Detroit was especially inclined to be affected by the nearby water bodies due to wind shifts. Days with lake breeze were selected using a protocol developed on the basis of weather information at Detroit Metropolitan Wayne County Airport, Detroit City Airport, Troy-Oakland Airport, Willow Run Airport, Grosse Ile Municipal Airport, a buoy on Lake St. Clair, another buoy on Lake Erie, and the Lafayette station operated by the Michigan Department of Environmental Quality—the latter data was obtained from the Michigan Department of Environmental Quality. The protocol involved considering land-water temperature differences, cloud cover, wind speed and wind direction. Details are provided in Appendix A.

2.2. Data analysis

The associations between temperature measurements and their attributes (space, time, imperviousness and distance-to-water) were assessed using the Kruskal–Wallis test, Pearson correlations- coefficients and linear regressions. Temperature measurements were summarized by daily mean, minimum and maximum temperatures, and the length of time that a given site registered temperatures above a threshold temperature. Longer duration of high temperatures may be more hazardous from a human-health perspective because it is difficult for people to recover from prolonged heat exposure. Curriero et al. (2002) have reported a daily mean temperature of 18.3 °C as a minimum temperature-mortality threshold for Chicago. We adopted this threshold in our analysis because Detroit and Chicago have a similar climate. We calculated the length of time (hours) above this threshold for each site per day, and then averaged that time length for each site.

2.3. Geostatistical models

Kriging is a geostatistical interpolation technique accounting for spatial correlation and it is used to predict or interpolate attribute values at unsampled locations given the information at sampled locations (Bailey and Gatrell, 1996). Spatial variation can be divided into two components: first-order variation (a trend component) and second-order effects (spatial dependence). First-order variation can be modeled using regression, which models observed values as a function of geocoordinates and secondary characteristics that are co-located with temperature measurements, and second-order effects can be estimated using the variogram, a function characterizing spatial correlation. Ordinary kriging only accounts for primary information, and assumes the variable of primary interest has a constant mean value. Universal kriging is a natural extension of ordinary kriging that includes location and other covariates in a regression model to estimate a trend for a primary variable (in our case, air temperature). Universal kriging relaxes the constant mean assumption used in ordinary kriging. Cokriging takes secondary information into account using a cross-variogram between primary and secondary variables. Cokriging usually works well when co-variables are strongly correlated and the secondary variable is more densely sampled compared with the primary variable.

Several kriging methods were used to interpolate the temperature measurements in this study. These methods include ordinary kriging, universal kriging with impervious surface and/or distance-to-water, and cokriging with impervious surface and/or distance-to-water. Each kriging technique was performed with and without removing the spatial trend of temperature measurements. A quadratic trend of the temperatures measured at HOBO locations was specified using x- and y-coordinates corresponding to longitude and latitude in the analysis. The performance of these kriging methods in predicting the actual temperatures measured at the HOBO sites was compared to the performance of a linear regression model where temperature was modeled as a function of impervious surface values or distance-to-water using the criteria described in the next section. Interpolation was applied to the 5:00 a.m., 5:00 p.m., and the daily mean temperature values each day. Exponential models were used in the variogram fitting for all kriging methods used in this study. The Gstat R package (Pebesma, 2004) and the R 2.7.2 software (R Development Core Team, 2006) were used in variogram estimations, interpolations, and subsequent evaluations.

2.4. Model evaluation

The performance of each interpolation procedure described above was evaluated and compared for each predicted temperature variable using cross validation. In this method, a measured temperature observation is temporarily removed from the dataset to which the model is fit, and this value is estimated from the remaining data using the same kriging method. This procedure is then repeated for all 17 temperature observations. The true and estimated values are then compared. We used the root mean square error (RMSE) statistic as the comparison criteria for this study, defined as:

$$\mathrm{RMSE}=\sqrt{\frac{1}{n}\sum_{i=1}^{n}(z_i-\hat{z}_i)^2} \quad (1)$$

where z_i is the temperature measurement at location i, $\hat{z}_i$ is estimated temperature value at location i, and n is number of the HOBO sites. Additionally, RMSE was used to examine whether interpolation could be improved by restricting the models to clear or cloudy days, and days with or without lake breezes. Moreover, we examined the associations between the RMSE and the correlations between temperature, impervious surface, and distance-to-water to facilitate the comparison.

2.5. Reconstructing spatial structure of temperature

Variograms describing the 800 × 800 m estimates across the Detroit metropolitan area derived from kriging were compared to those calculated from temperatures measured at the 17 HOBO sites. Variograms enable us to determine the spatial dependence of temperature in the study area. We chose the three hottest days (August 18th, 22nd, and 23rd, 2010) during the study period for this exercise. Kriging predictions were estimated from ordinary kriging, universal kriging with impervious surface, and cokriging with impervious surface values. If variograms derived from the predictions using impervious surface had smaller estimated correlation ranges (i.e., if the patterns were less smooth) than those from the temperature measures alone, this would suggest that impervious surface value could be helpful in reconstructing finer-scale spatial-structure of temperature.

3. Results

3.1. Descriptive statistics

Descriptive statistics for the HOBO temperature measurements at the 17 sites are shown in Table 1. The maximum temperature values at 17 sites during 22 days had the largest range (32.9–36.1 °C), followed by minimum (8.3–12.3 °C) and mean temperature observations (20.5–21.9 °C). For the entire period, the Kruskal–Wallis test showed that the temperature time series at the 17 sites were significantly different from each other (p<0.001), indicating that the patterns of temporal variation in temperature varied across the metropolitan area.

In general, the largest spatial variation in temperatures between stations occurred in the daily 5:00 p.m. temperatures, followed by the 5:00 a.m. and daily mean temperature records (Fig. 2). This finding was also indicated by the averages of daily interquartile range (IQR) and range of these three metrics: for daily 5:00 p.m., average IQR and range were 1.7 and 4.0

°C, respectively; for daily 5:00 a.m., average IQR and range were 1.3 and 3.4 °C, respectively; and for daily mean temperature, they were 0.6 and 1.7 °C, respectively. The spatial variability of these three indicators also varied by day of study. For example, for the three hottest days (August 18th, 22nd and 23rd) in this period, the 5:00 a.m. measurements had the largest variability, followed by the daily mean and the 5:00 p.m. records. However, for the coldest day (August 10th), the 5:00 am observations still had the largest variation, followed by the 5:00 p.m. and daily mean values.

The average of daily mean temperature during the study period had the strongest association with the percent impervious surface in the 800 m cell within which each of the 17 HOBO sites fell, followed by the average of daily minimum values and the average of daily maximum values (Supplemental Figure 1). Regression diagnostics on temperatures against percent impervious surface showed that two assumptions of linear regression models (residuals having normal distribution and constant variance) were reasonably met. Pearson's correlation coefficient (r) for percent impervious surface and average of daily mean temperatures was 0.75 (95% confidence interval (CI):0.42, 0.90). The linear effect coefficient for the percent impervious surface was 0.02 (95% CI: 0.01, 0.03), which represented a 0.02 °C temperature increase with each percent increase in imperviousness. Correlations between impervious surface and the average of daily minimum temperatures were somewhat lower, with a coefficient of 0.59 (95% CI: 0.15, 0.83). But the linear effect coefficient (0.04; 95% CI: 0.01, 0.07) for impervious surface against average daily minimum temperature was higher than the corresponding coefficient for mean temperature. However, the average of daily maximum temperature was not statistically correlated with percent imperiousness (r= −0.10, 95% CI: −0.56, 0.40; linear effect coefficient= −0.01, 95% CI: −0.05, 0.03). Additionally, impervious surfaces did not have a significant effect (0.01; 95% CI: −0.02, 0.03) on the duration of high temperatures, as indicated in Supplemental Figure 1D.

Distance-to-water had the strongest associations with the average daily minimum, followed by the averages of daily maximum and mean, temperatures during the study period (Supplemental Figure 2). Diagnostic plots on the regressions showed that two assumptions of linear regression models (normal distribution and constant variance) were satisfied. Correlation coefficients between the distance-to-water and the temperature measures (daily minimum, maximum, mean temperatures, and the length of time over the threshold) were −0.86 (95% CI: −0.95, −0.64), 0.61 (95% CI: 0.19, 0.85), −0.48 (95% CI: −0.78, 0.01), and −0.25 (95% CI: −0.65, 0.27), respectively. Linear effect coefficients, which represent the magnitude of temperature/length change with an one kilometer increase in distance, were −0.08 (95% CI: −0.10, −0.06), 0.06 (95% CI: 0.02, 0.10), −0.02 (95% CI:−0.04, 0.00) and −0.01 °C km^{-1} (95% CI: −0.05, 0.02), respectively.

3.2. Evaluation of kriging methods

Kriging methods generally had slightly better performance (indicated by smaller RMSEs) than the linear regression method with imperviousness for daily 5 a.m./p.m. temperature metrics, and than the linear regression with distance-to-water for daily average temperature. Kriging methods performed similarly to these two linear regression models under other

cases for three temperature metrics (Fig. 3A–C). All kriging methods had a similar performance, except for cokriging with imperviousness and distance-to-water, and kriging methods with detrending performed similarly to those without detrending. Adding secondary information in addition to detrending did not improve performance greatly. The best performance of all methods was seen for models of daily mean temperature, followed by daily 5 a.m. and 5 p.m. temperature.

The performance of all methods varied not only with temperature metric and method type, but under clear and cloudy conditions also (Fig. 4A–C). For the daily 5 p.m. temperature (Fig. 4C), kriging during clear days had slightly better performance compared to cloudy days. However, different trends were seen in the daily 5 a.m. (Fig. 4A) and mean temperatures (Fig. 4B). For daily 5 a.m. temperature, kriging using only clear days had worse performance compared to analysis using the cloudy days. For the daily mean temperature, kriging predictions were similar among different kriging methods and did not differ much when models were stratified by clear or cloudy days.

For the daily 5 p.m. temperature, all kriging methods except for cokriging with impervious surface values and distance-to-water improved performance slightly on days with a lake breeze (Fig. 4F). However, the linear regression model with imperviousness showed worse performance on days with a lake breeze, and distance-to-water performed similarly under the two conditions. Moreover, for the daily 5 a.m. and daily mean temperatures (Fig. 4D–E), all kriging methods did not have a consistent pattern.

3.3. Temperature spatial structure reconstruction

The variograms derived from the temperature measurements and kriging predictions illustrate that cokriging-derived variograms had the shortest ranges, followed by universal kriging-derived variograms, ordinary kriging-derived variograms, and original variograms based on temperature at 17 sites (Table 2).

4. Discussion

The urban climate literature has generally not addressed whether satellite-derived imperviousness information can improve the predictions of temperature at unsampled locations and capture the fine-scale spatial structure of temperature in a large area. In the Detroit Metropolitan region, we had an opportunity to investigate whether land use (imperviousness) and meteorological conditions (cloud cover and lake breezes) can improve the temperature predictions. We summarize our key findings in the next paragraph and next talk in detail about some of them.

Temperatures measured at the 17 sites were statistically significantly different from each other, consistent with a Phoenix, Arizona study, which measured temperature in eight city neighborhoods during the summer of 2003 (Harlan et al., 2006). Kriging models had generally slightly better prediction performance than linear regression models, and impervious surface values and distance-to-water generally improved predictions slightly. The influences of nearby imperviousness and water bodies on temperature depended on temperature metrics, and the largest impacts of both occurred for daily minimum

temperature compared to other metrics. Also, in general, for daily 5 p.m. temperature, kriging models performed slightly better under days with lake breezes and with less cloud cover. Finally, we found that incorporating high-resolution impervious surface information into cokriging or universal kriging was helpful for characterizing fine-scale spatial structure of temperature.

The associations between the temperature metrics and imperviousness or distance-to-water could be explained by their physical mechanisms. The positive effect coefficients of temperature-imperviousness are indicative of greater absorption and irradiance by impervious surfaces compared to vegetated surfaces, leading to higher mean and minimum temperature values. The associations for imperviousness imply that, for the lows and means, nearby imperviousness is a key factor in defining the local environment because of the heat capacity of the impervious surface; for the highs, factors other than imperviousness influence the temperature. The associations for distance-to-water may be mainly explained by water-body effects. Water is warmer than land at night, and is cooler than land in the daytime. Thus, HOBO stations closer to a lake or other water body would be expected to have a higher minimum temperature and lower maximum temperature.

Kriging performance varied with temperature metrics. Kriging methods performed slightly better or similarly to linear regression models because, although kriging methods account for local temperature measurements in the estimation, the number (n=17) of HOBO sites is limited. Smaller RMSE associated with daily mean temperature compared to the other two metrics might be explained by the smaller spatial variation in daily mean temperature compared to the other two temperature parameters.

Different patterns of performance on temperature metrics under clear/cloudy conditions could be attributed to two factors. First, clearness was defined during daytime, and is a surrogate of sunniness and is thus intuitively less likely to affect the daily 5 a.m. temperature, which occurs before dawn. Second, the stratification by clear/cloudy days did not improve kriging performance for daily mean temperature mainly because clear days can result in higher temperatures in the day due to heating by the sun’s rays, and lower temperatures at night if skies remain clear, since clouds are not trapping the daytime heat. The result of averaging these temperatures over a 24-hour period would be expected to be approximately the same as for cloudier days where the daily minimum and maximums would be expected to be less extreme at both ends of the range.

The patterns of kriging performance on days with and without a lake breeze could be explained by the fact that lake breeze was defined according to daytime weather information. The changing patterns under lake-breeze stratification for daily 5 p.m. temperature were probably due to stronger spatial correlation on lake-breeze days, kriging accounting for spatial correlation, as well as linear regression models not taking spatial correlation into account. Also, correlations with impervious surfaces might be expected to be lower on breezy days, because the associated advection would reduce temperature differences due to local surface characteristics.

Strong correlations between the temperature metrics and imperviousness or distance-to-water did not enhance the performance (indicated by smaller RMSEs) of either cokriging or universal kriging models for most cases (Supplemental Figures 3–5). Goovaerts (2000) suggested that cokriging estimates are affected by the correlation between primary and secondary information as well as their spatial continuity patterns. These findings suggested that cokriging performance in this case study was mainly determined by the latter.

In general, the performance of all the kriging methods decreased with increased variance in temperature (Supplemental Figures 6–8). These findings are consistent with Collins and Bolstad (1996), and might be attributable to the increased difficulty of making estimates when the values on which those estimates are based are more variable.

Shorter correlation ranges (Table 2) in temperature estimates indicated more textured spatial patterns, suggesting that cokriging or universal kriging were better able to recreate some of the fine-scale spatial structure of temperature by including satellite-derived impervious surface values than were estimates based only on our limited direct measurements of temperature.

Remotely sensed data have the disadvantage of temporal coverage constrained by the observing time of satellites, although they have the primary advantage of providing large spatial coverage and resolution of surface temperature and land-cover characteristics. In this study, we used the latest NLCD 2006 impervious surface data, but they did not exactly match the timing of the HOBO study conducted in 2008. We compared the percent impervious surface at the 17 HOBO sites derived from the NLCD 2006 and the NLCD 2001 version 2 imperviousness datasets (USGS, 2011). There were no differences except for at two sites (changes were +1% and +6%, respectively). We also conducted a sensitivity analysis using the NLCD 2001 version 1 impervious surface data, which were calculated using different algorithms compared to the recently available the NLCD 2006 and the NLCD 2001 version 2 datasets (USGS, 2011). The differences of monitors' imperviousness between the 2006 and 2001 version 1 ranged from −15% and +26% with a median value of −4%. We found that the quantitative results changed slightly, but our major conclusions were not affected. Thus, these findings suggested that imperviousness around the monitors generally changed slowly and did not significantly affect our major conclusions.

Besides the mismatch between the timings of the imperviousness and temperature measurements, the study had a few other limitations. First, our secondary variables included only imperviousness and distance-to-water. The imperviousness was estimated using remotely sensed data, and the distance-to-water was approximated as the shortest straight-line distance between a HOBO site and its nearest water body. The analysis did not account for land-use types, vegetation, urban morphology and buildings around HOBO monitors. Second, the relative small number of monitors reduced the power of the data analysis. Third, the study period was relatively short, and did not cover extremely hot days.

5. Conclusions

A set of HOBO temperature sensors was used to characterize spatial variability of summertime temperature in the Detroit metropolitan area, Michigan, USA. Several kriging

methods (ordinary kriging, cokriging and universal kriging) were compared, and results suggested that secondary information such as percent impervious surface, lake breezes and cloud cover generally improved model performance slightly when using a limited set of temperature measurements. Additionally, our investigation showed that impervious surface values could allow us to reconstruct fine-scale spatial structure of temperature. Considering the high resolution of satellite-derived impervious information, these findings have implications for detecting higher temperature areas, which can be combined with socio-demographic information to identify 'hot spots' of vulnerability. These findings also suggested the potential of imperviousness as a temperature surrogate for heat-related epidemiological studies, but further studies are needed to evaluate its performance within the context of epidemiology.

Supplementary Material

Refer to Web version on PubMed Central for supplementary material.

Acknowledgments

The research described in this paper was funded by support of the Graham Environmental Sustainability Institute at the University of Michigan; the U.S. Environmental Protection Agency Science to Achieve Results (STAR) grant R832752010; and the U.S. Centers for Disease Control and Prevention grant R18 EH 000348.

This paper does not necessarily reflect the views of these organizations. The authors appreciate the suggestions of Dr. Anna Michalak in the Department of Civil and Environmental Engineering at the University of Michigan, data support by Mr. Craig Fitzner (MDEQ), and scientific and administrative support by Dr. Frank Marsik in the Department of Atmospheric, Oceanic, and Space Science at the University of Michigan.

References

Anderson BG, Bell ML. Weather-related mortality: how heat, cold, and heat waves affect mortality in the United States. Epidemiology. 2009; 20 (2):205–213. [PubMed: 19194300]

Bailey, T.; Gatrell, T. Interactive Spatial Data Analysis. Prentice Hall; 1996. p. 183-217.

Brazel A, Selover N, Vose R, Heisler G. The tale of two climates—Baltimore and Phoenix urban LTER sites. Clim Res. 2000; 15 (2):123–135.

Collins, FC.; Bolstad, PV. [accessed 25/5/2010] A Comparison of Spatial Interpolation Techniques in Temperature Estimation. 1996. See ⟨http://www.ncgia.ucsb.edu/conf/SANTA_FE_CD-ROM/sf_papers/collins_fred/collins.html⟩

Curriero FC, Heiner KS, Samet JM, Zeger SL, Strug SL, Patz JA. Temperature and Mortality in 11 Cities of the Eastern United States. Am J Epidemiol. 2002; 155:80–87. [PubMed: 11772788]

Degaetano AT, Belcher BN. Spatial interpolation of daily maximum and minimum air temperature based on meteorological model analyses and independent observations. J Appl Meteorol. 2006; 46:1981–1992.

Goovaerts P. Geostatistical approaches for incorporating elevation into the spatial interpolation of rainfall. J Hydrol. 2000; 228:113–129.

Harlan SL, Brazel AJ, Prashad L, Stefanov WL, Larsen L. Neighborhood microclimates and vulnerability to heat stress. Soc Sci Med. 2006; 63:2847–2863. [PubMed: 16996668]

Houet T, Pigeon G. Mapping urban climate zones and quantifying climate behaviors e An application on Toulouse urban area (France). Environ Pollut. 201110.1016/j.envpol.2010.12.027

Im H, Rathouz PJ, Frederick JE. Space–time modeling of 20 years of daily air temperature in the Chicago metropolitan region. Environmetrics. 2009; 20:494–511.

Johnson DP, Wilson JS, Luber GC. Socioeconomic indicators of heat-related health risk supplemented with remotely sensed data. Int J Health Geogr. 2009; (1):57–70. [PubMed: 19835578]

Kestens Y, Brand A, Fournier M, Goudreau S, Kosatsky T, Maloley M, Smargiassi A. Modelling the variation of land surface temperature as determinant of risk of heat-related health events. Int J Health Geogr. 2011; 10 (1):7–15. [PubMed: 21251286]

Loubier, JC. Optimizing the interpolation of temperatures by GIS: A space analysis approach. In: Dobesch, H.; Dumolard, P.; Dyras, I., editors. Spatial Interpolation for Climate Data: The Use of GIS in Climatology and Meteorology. Vol. 2010. ISTE Ltd; London: 2007. p. 97-108.

Luo Z, Wahba G, Johnson DR. Spatial–temporal analysis of temperature using smoothing spline ANOVA. J Clim. 1998; 11:19–28.

National Climatic Data Center (NCDC). [accessed 13/12/2008] NOAA Satellite and Information Service. 2008. See ⟨http://www.ncdc.noaa.gov/oa/climate/isd/index.php?name=isd-lite⟩

National Research Council. Earth Science and Applications from Space: National Imperatives for the Next Decade and Beyond. National Academies Press; Washington, DC: 2007.

Ninyerola M, Pons X, Roure JM. A methodological approach of climatological modelling of air temperature and precipitation through GIS techniques. Int J Climatol. 2000; 20:1823–1841.

Oka M. The influence of urban street characteristics on pedestrian heat comfort levels in Philadelphia. Trans GIS. 2011; 15 (1):109–123.

O'Neill MS, Zanobetti A, Schwartz J. Modifiers of the temperature and mortality association in seven US cities. Am J Epidemiol. 2003; 157 (12):1074–1082. [PubMed: 12796043]

O'Neill MS, Zanobetti A, Schwartz J. Disparities by race in heat-related mortality in four U.S. cities: the role of air conditioning prevalence. J Urban Health. 2005; 82 (2):191–197. [PubMed: 15888640]

Oswald E, Rood R, Zhang K, Gronlund C, O'Neill M, White-Newsome J, Brines S, Brown D. An investigation into the spatial variability of near-surface air temperatures in the Detroit, MI metropolitan region. J Clim Appl Meteorol. submitted for publication.

Pebesma EJ. Multivariable geostatistics in S: the gstat package. Comput Geosci. 2004; 30:683–691.

R Development Core Team. R: A Language and Environment for Statistical Computing. R Foundation for Statistical Computing; Vienna, Austria: 2006. See http://www.R-project.org [accessed 2/12/2008]

Schulz A, Northridge ME. Social determinants of health: implications for environmental health promotion. Health Educ Behav. 2004; 31 (4):455–471. [PubMed: 15296629]

Schwartz J, Samet JM, Patz JA. Hospital admissions for heart disease: the effects of temperature and humidity. Epidemiology. 2004; 15 (6):755–761. [PubMed: 15475726]

U.S. EPA. [accessed 24/7/2010] Reducing Urban Heat Islands: Compendium of Strategies. 2008. ⟨http://www.epa.gov/heatisland/resources/pdf/BasicsCompendium.pdf⟩

U.S. Geological Survey. [accessed 12/4/2011] National Land Cover Database (NLCD 2006) NLCD 2006 Percent Developed Imperviousness. 2011. See ⟨http://gisdata.usgs.gov/TDDS/DownloadFile.php?TYPE=nlcd2006&FNAME=NLCD2006_impervious_2-14-11.zip⟩

Vicente-Serrano SM, Saz-Sánchez MA, Cuadrat JM. Comparative analysis of interpolation methods in the middle Ebro Valley (Spain): application to annual precipitation and temperature. Clim Res. 2003; 24 (2):161–180.

Vogt JV, Viau AA, Paquet F. Mapping regional air temperature fields using satellite derived surface skin temperatures. Int J Climatol. 1997; 17:1559–1579.

Wilhelmi OV, Purvis KL, Harris RC. Designing a geospatial information infrastructure for mitigation of heat wave hazards in urban areas. Nat Hazards Rev. 2004; 5 (3):147–158.

Appendix A. Supplementary Information

Supplementary data associated with this article can be found in the online version at doi: 10.1016/j.envres.2011.08.012.

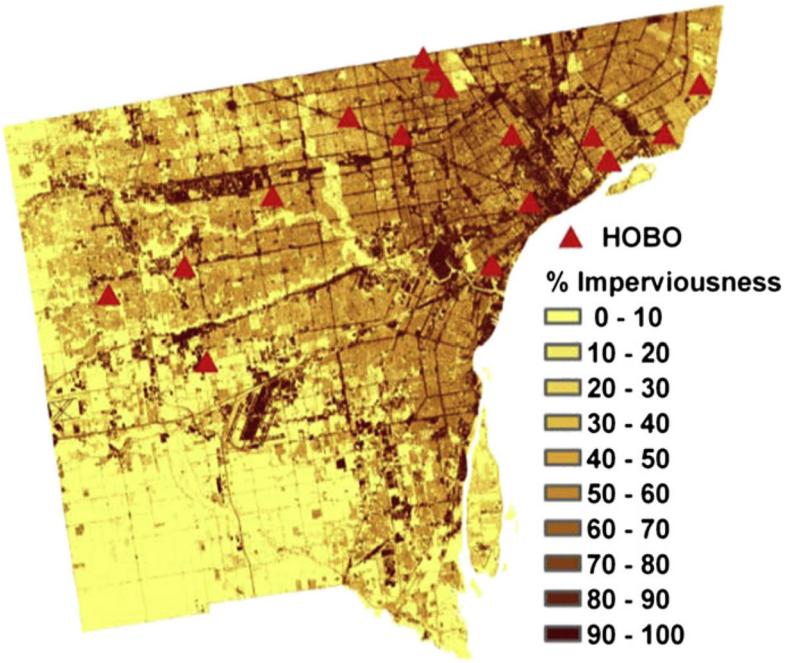

Fig. 1.

HOBO sites in the Detroit metropolitan area, Michigan, USA (HOBO sites in triangles with impervious surface image as the background).

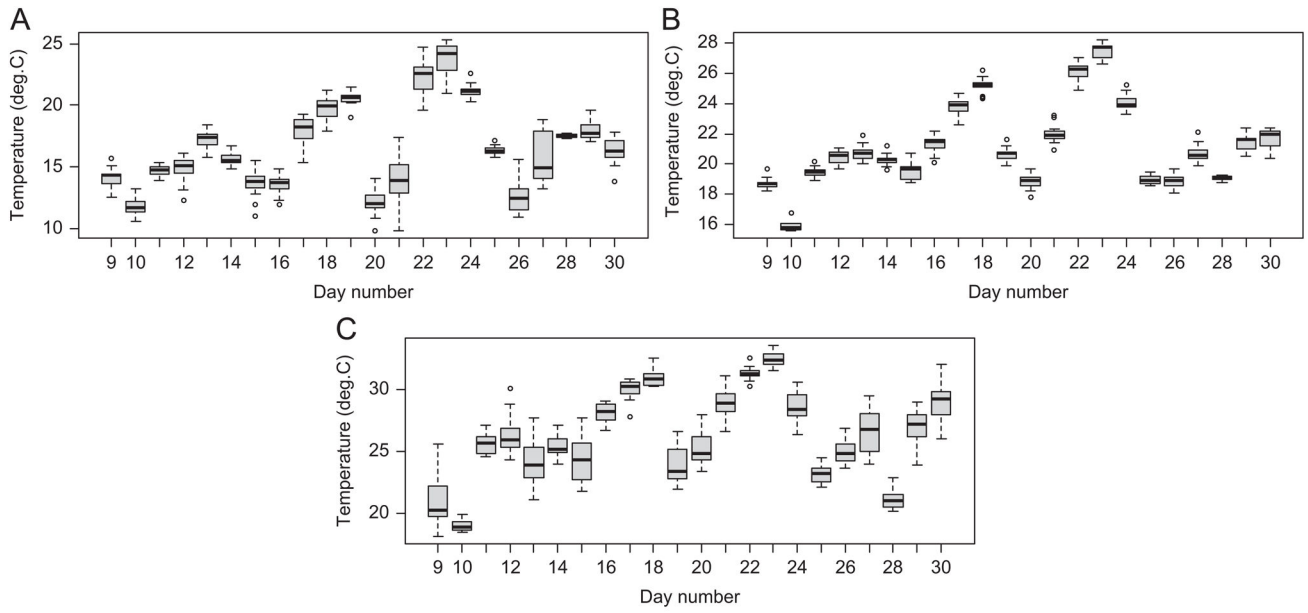

Fig. 2.

Spatial and temporal variability of the temperature observations (Each box plot shows the spatial variability across the 17 stations on a given day). (A) Daily 5:00 a.m. temperature; (B) daily mean temperature and (C) daily 5:00 p.m. temperature.

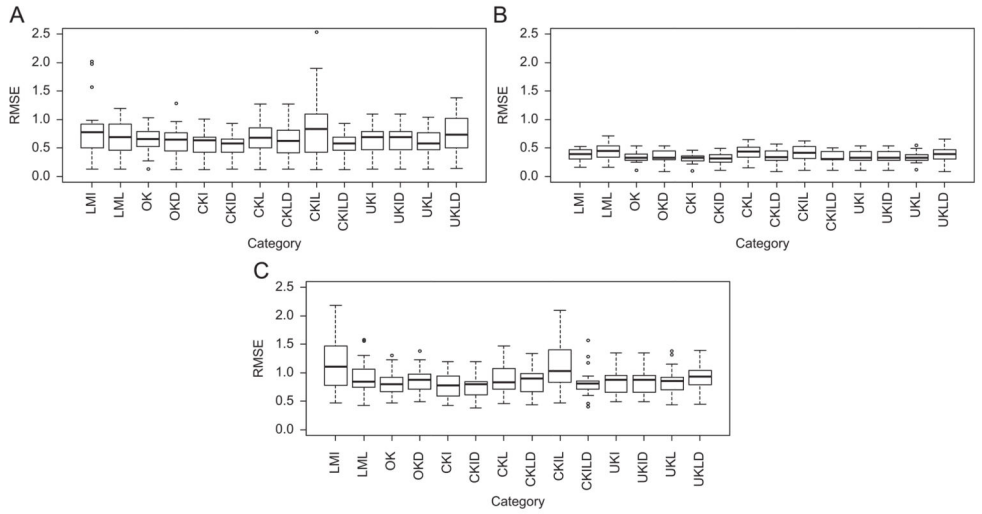

Fig. 3.

Model comparison between different kriging and linear regression methods (RMSE, root mean square error; LMI and LML, temperature was modeled as a function of impervious surface values or distance-to-water; OK, ordinary kriging; OKD, ordinary kriging with detrending; CKI, cokriging with impervious surface values; CKID, cokriging with impervious surface values and detending; CKL, cokriging with distance-to-water; CKLD, cokriging with distance-to-water and detending; CKIL, cokriging with impervious surface values and distance-to-water; CKILD, cokriging with impervious surface values, distance-to-water and detending; UKI, universal-kriging with impervious surface values; UKID, universal-kriging with impervious surface values and detrending; UKL, universal-kriging with distance-to-water; UKLD, universal-kriging with distance-to-water and detrending). (A) Daily 5:00 a.m. temperature; (B) daily mean temperature and (C) daily 5:00 p.m. temperature.

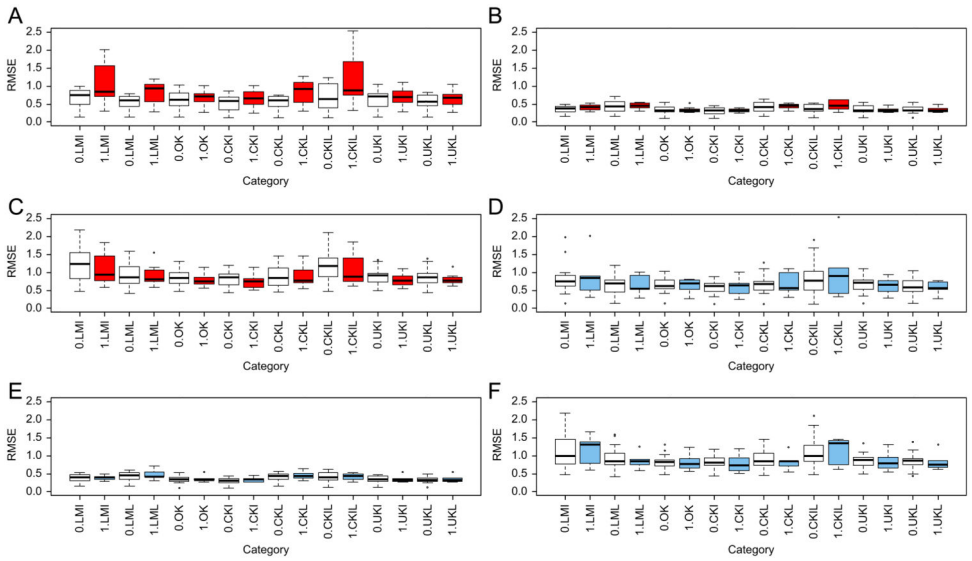

Fig. 4.

Model comparison between different kriging and linear regression methods under clear/cloudy days or with/without a lake breeze. (A–C, days were stratified as clear days (1 on the *X* axis) and cloudy days (0 on the *X* axis); D–F, one and zero representing days with and without lake breeze; Otherwise as Fig. 3). (A) Daily 5:00 a.m. temperature under clear and cloudy days; (B) daily mean temperature under clear and cloudy days; (C) daily 5:00 p.m. temperature under clear and cloudy days; (D) daily 5:00 a.m. temperature with/without a lake breeze; (E) daily mean temperature with/without a lake breeze; (F) daily 5:00 p.m. temperature with/without a lake breeze.

Table 1

Data summary of the temperature measurements at 17 sites, Detroit, Michigan, USA (August 9th to August 30th, 2008; Temperature units are in degrees Celsius).

NO.	Site name	*N*	Mean	SD[a]	Min	P25[b]	Median	P75[c]	Max
1	Boston Edison	6336	21.3	4.5	11.6	18.0	21.1	24.4	32.9
2	Canton	6336	20.5	5.5	8.3	16.2	20.5	24.9	33.7
3	Corktown	6336	21.4	4.9	10.6	17.9	21.1	24.8	34.3
4	Delray	6336	21.9	4.4	12.3	18.7	21.9	25.1	33.0
5	East Detroit	6336	21.5	4.9	11.8	17.8	21.2	24.8	34.5
6	East Jefferson	6336	20.8	4.4	11.2	17.7	20.7	23.6	32.9
7	Grosse Point Farms	6336	20.8	4.4	10.8	17.5	20.5	23.9	34.1
8	Indian Village	6336	21.2	4.8	10.9	17.6	20.9	24.4	34.1
9	West Village	6336	21.1	4.6	11.5	17.6	21.1	24.3	33.3
10	Redford	6336	21.3	5.5	10.7	17.1	20.9	25.6	36.1
11	Romulus	6336	20.7	5.6	9.9	16.3	20.5	25.0	34.7
12	West Detroit 1	6336	21.2	4.9	10.7	17.4	21.1	24.7	34.3
13	West Detroit 2	6336	21.4	5.2	10.7	17.3	21.0	25.4	35.0
14	West Detroit 3	6336	21.0	5.1	10.6	16.9	20.7	24.9	34.5
15	West Detroit 4	6336	21.1	5.2	10.5	17.1	20.8	25.1	35.1
16	West Detroit 5	6336	21.3	5.4	10.1	17.1	21.0	25.5	35.0
17	Westland	6336	20.8	5.2	10.4	16.8	20.4	24.8	33.9

[a] Standard deviation.

[b] 25th percentile values.

[c] 75th percentile values.

Table 2

Estimated correlation ranges (in kilometers) from semivariograms derived from different kriging models for three different temperature metrics during three August days in 2008; Detroit, Michigan, USA.

Type	August 18th			August 22nd			August 23rd		
	5 a.m.	Mean	5 p.m.	5 a.m.	Mean	5 p.m.	5 a.m.	Mean	5 p.m.
OK [a]	17.9	6.1	2.7	17.2	65.1	4.1	14.5	6.4	18.1
OK_PRED[b]	10.3	4.9	4.9	10.3	4.9	4.9	14.8	4.9	4.9
CK_PRED[c]	2.0	2.4	2.1	2.3	2.4	2.3	2.0	2.1	2.4
UK_PRED[d]	10.3	4.9	4.9	5.9	4.9	4.9	12.3	4.9	4.9

[a] OK, ordinary kriging based on 17 HOBO sites.

[b] OK_PRED, ordinary kriging based on the prediction across the study region derived from ordinary kriging.

[c] CK_PRED, cokriging based on the prediction across the study region derived from cokriging with imperviousness.

[d] UK_PRED, universal kriging based on the prediction across the study region derived from universal kriging with imperviousness.